Royal Netherlands
Meteorological Institute
Ministry of Infrastructure and the Environment

Inverting ground-based polarisation lidar measurements to retrieve cloud microphysical properties during the Ascension Island Initiative

Jessica Brown

KNMI Internal Report IR-2016-10

Koninklijk Nederlands
Meteorologisch Instituut
Ministerie van Infrastructuur en Milieu

Internship Report

Inverting ground-based polarisation lidar measurements to retrieve cloud microphysical properties during the Ascension Island Initiative

Jessica Brown
October, 2016

Wageningen University
Meteorology and Air Quality Department

supervised by
Martin de Graaf
Folkert Boersma

WAGENINGEN UNIVERSITY
WAGENINGEN UR

Contents

Abstract

The interaction between clouds and aerosols, and the resulting impact on radiative forcing is one of the most uncertain mechanisms in the global climate system. To gain a better understanding of these important interactions a number of international campaigns have taken place in the southeastern Atlantic region in 2016. This region is characterised by a consistent layer of marine boundary layer stratocumulus clouds, capped by a temperature inversion created by widespread subsidence. Large biomass burning events in the southern African dry season lead to high concentrations of aerosols being advected across and above these cloud layers. This region has often been described as a 'natural laboratory' for examining cloud and aerosol interactions.

Here we present the first results from the Ascension Island Initiative (ASCII) campaign. The ASCII campaign was conducted on Ascension Island in September 2016, with the aim to investigate the effect of biomass burning aerosols on cloud microphysical properties using a ground-based UV depolarisation lidar. Observations from the lidar were processed using an inversion method which produces estimates of cloud microphysical properties such as the effective radius and cloud droplet number density. This new inversion method is based utilising lookup tables based on Monte Carlo modelling of multiple scattering within idealised semi-adiabatic clouds. Conditions over Ascension Island in September were characterised by a persistent deck of stratocumulus, topped by a strong temperature inversion at around 1 to 1.5 km. Aerosols were visible on 19 out of 25 of the campaign days, with the aerosol layer ranging between 1.5 to 4 km in altitude. The average cloud number density found was between 400-600 cm^{-3} while the average effective radius near the cloud base was between 3.4 to 4.2 μm. Preliminary evidence for the indirect cloud-aerosol effect is seen, with a decrease in the effective radius and increase in the number density in cases when the aerosol layer occurs directly above the peak attenuated backscatter. The inversion method did provide a robust method to quickly observe cloud microphysical properties of stratocumulus clouds over Ascension. However, as no lidar calibration coefficients are known for the ASCII dataset as of yet, the inversion products should be treated with caution, with errors expected to be greater than 30%. In addition, the inversion method itself has yet to be verified.

1 The Ascension Island Initiative

The Ascension Island Initiative (ASCII) campaign took place between September 1$^{\text{st}}$ to 30$^{\text{th}}$ 2016 on Ascension Island. This campaign was a joint initiative between KMNI and TU Delft, with Martin de Graaf as the primary investigator.

The aim of the ASCII campaign was to identify whether the microphysical properties of marine stratocumulus clouds altered with the presence of aerosols. To achieve this a depolarisation UV lidar was set up on Ascension during September, 2016. This time period was selected as it is a period of high smoke presence as well as to coincide with a period of intensive observations from a number of other international campaigns including LASIC, CLARIFY (now postponed until 2017) and NASA-ORACLES, all of which also focus on understanding and investigating the interaction of biomass burning smoke and clouds in the southeastern Atlantic region. A brief introduction to these other campaigns is given in Appendix A.

Ascension Island is a remote, volcanic island located at 8°S 14°W, 1600 km from Africa and 2250 km off the coast of Brazil (Fig. 1). It is governed by the UK and is home to a British Royal Airforce base as well as a United States Airforce base. The climate of Ascension is classed as a tropical desert, with temperatures ranging from 22 to 31 °C. The annual rainfall is very low at around 140 mm annually, with peak rainfall occurring in April. The prevailing winds come from the south east (Zuidema et al., 2016). The island is formed from an underwater volcano which emerged from the ocean just 1 million years ago.

Figure 1: Image from Google Maps showing the location of Ascension Island, given by the yellow cross, and St Helena, given by the orange star, in between the coasts of east Africa and Brazil. St Helena was the location of smaller LASIC observational site.

2 Biomass burning aerosols and their transport

African fires are responsible for an average of 30-50% of the total amount of vegetation burned globally each year, being the largest single source of biomass burning (Roberts et al., 2009). Roberts et al. (2009) estimate that in 2004, 855 million tonnes of biomass was burned in open vegetation fires over the continent of Africa. In southern Africa most burning occurs during the dry season between

April to October (Fig. 2), with fires used for agricultural reasons and to clear land (Sinha et al., 2003; Anderson et al., 1996). In addition in more remote areas, many fires are started by lightening accompanying spring rains (Swap et al., 1996).

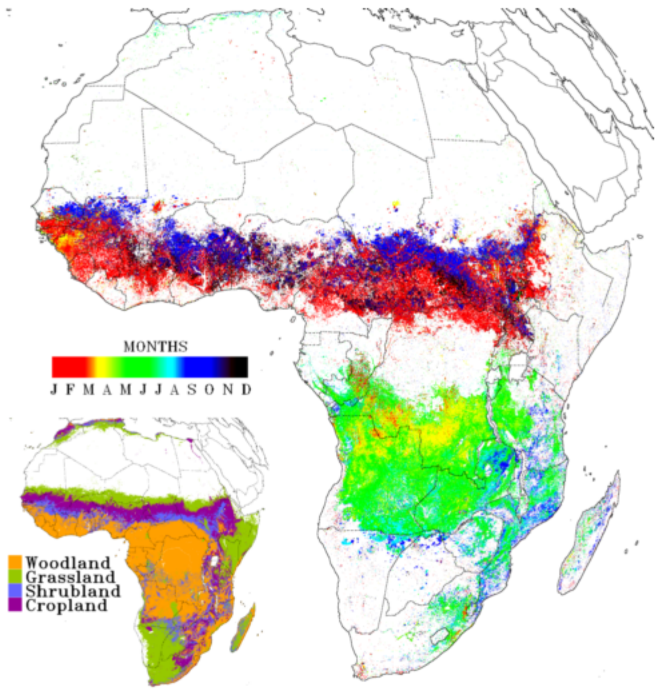

Figure 2: Active fires over Africa for 2004, colour-coded by day of detection. Inset map: Global Land Cover 2000 land cover map aggregated into four broad land cover classes. Taken from Roberts et al. (2009).

As seen in Figure 3, anticyclonic circulations dominate circulation patterns over the subcontinent during the dry season. In addition, southern Africa and the subtropical Atlantic are located in a region of large-scale subsidence due to the meeting of the southern hemisphere Hadley and Ferrel circulation cells (Garstang et al., 1996). The vertical profile of the atmosphere over the Atlantic is characterised by the persistent presence of multiple stable layers, with a trade wind inversion being found at 1 km. A higher subsidence inversion is generally found at 5 to 6 km (Fuelberg et al., 1996). These stable layers act to limit vertical mixing between the boundary layer (below the trade wind inversion) and the less stable air in the middle troposphere (Fuelberg et al., 1996).

Aerosols which end up over Ascension typically begin by mixing in the deep boundary layer over southern Africa, with vertical mixing into the troposphere being prevented by persistent continental stable layers at 700 to 500 hPa (Sinha

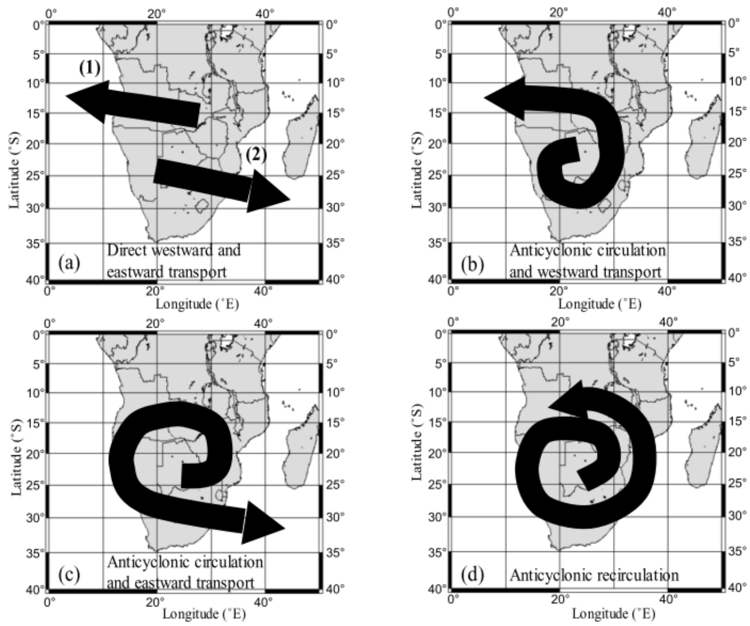

Figure 3: Five main synoptic tropospheric air transport pathways over southern Africa during the dry season. Taken from (Sinha et al., 2004)

.

et al., 2003). This air is then pushed up over cooler air from rainforests in the central Congo before being transported between the two inversion layers by the easterly winds from the anticyclonic flows to accumulate over the southeastern Atlantic (Sinha et al., 2003). Typically aerosols are located in a layer between 2-4 km (Wilcox, 2010). Swap et al. (1996) found that the transport of aerosols took between 5-9 days between the Namibian coast and Ascension Island. In addition to biomass burning aerosols they also recorded the transport of dust particles.

In addition to finding aerosols above the trade wind inversion, Swap et al. (1996) also found aerosols at low altitudes, representing aerosols originating from different locations within Africa which had penetrated the stable layers to different degrees over the continent. In addition, Anderson et al. (1996) suggests that the widespread subsidence over the Atlantic may lead to the mixing of the aerosol layer and boundary layer clouds with prolonged transport, such as transport to Ascension Island.

3 Clouds over the southeast Atlantic

The typical clouds found in subtropical marine regions, such as around Ascension Island, are low lying bands of stratocumulus capping the boundary layer and are typically found between 1-1.5 km. These marine stratocumulus clouds are very important for the global climate, as they have a high albedo compared to the dark ocean over which they occur and reflect around 30% of the incoming solar radiation (Bennartz, 2007). An estimated 4% increase in their cover could offset the warming due to a doubling of CO_2 (Albrecht et al., 1988).

These clouds are associated with large-scale subsidence over a cool ocean (Paluch et al., 1991). These conditions lead to a strong temperature inversion at the top of the boundary layer, through which clouds are not able to penetrate, leading to expansive decks of stratocumulus clouds. They are maintained by turbulent mixing due to longwave cooling at the cloud top and are sustained by a balance between moisture supply from the ocean surface and the entrainment of dry air from the troposphere (Bennartz, 2007). This longwave cooling at the cloud top also enhances the strength of the inversion layer (Paluch et al., 1991). They are typically accompanied by light drizzle. As these clouds are so important in modulating the Earth's climate, any interactions which they have with aerosols are also very important in regulating the earth-atmosphere system.

4 Interactions between clouds and aerosols

The numerous and complex ways in which aerosols can influence clouds, as well as the representation of cloud processes in climate models has been recognized as a dominant source of uncertainty in our understanding of changes to the climate system (Boucher et al., 2013). Aerosols have been identified to have three main pathways in which they influence the earth-atmosphere system; firstly aerosols can scatter or absorb solar radiation, secondly they can scatter or absorb thermal radiation and thirdly aerosols can act as cloud condensation nuclei (CCN) or ice nuclei (IN) (Lohmann and Feichter, 2005).

4.1 Aerosols above clouds: The semi-direct effect

In the case of the southeastern Atlantic, the aerosols from biomass burning are mostly found in a thick layer between 2-4 km, while the low marine stratocumulus are usually found at heights of less than 1.5 km (Wilcox, 2010). This separation of clouds and aerosols limits this cloud-albedo effect as aerosols are not available in the boundary layer to act as additional CCN, and leads to a different pathway for cloud-aerosol interactions. Here, aerosols mainly influence clouds by changing the radiative balance and temperature profile of the atmosphere. The thick layer of aerosols above the clouds absorbs radiation, substantially decreasing the downward solar radiation reaching the boundary layer, cooling the surface and warming the troposphere (Wilcox, 2010). This warming

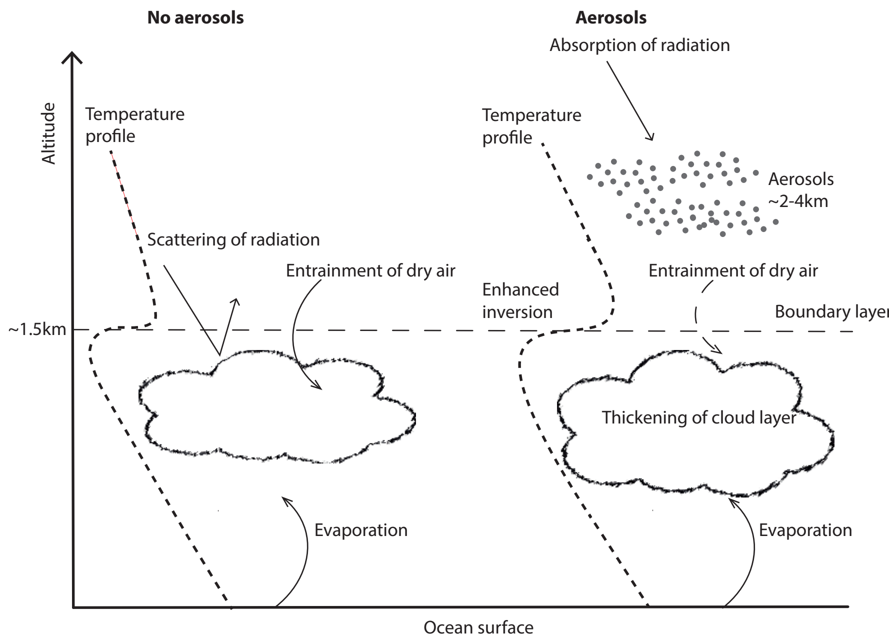

Figure 4: Diagram indicating the expected semi-direct effect of the presence of an overlying aerosol layer on marine boundary layer stratocumulus clouds

of air within the aerosol layer increases the buoyancy of free-troposphere air, strengthens the boundary layer temperature inversion and reduces entrainment of dry air into the boundary layer and cloud top.

Numerous studies have examined the effect of an above-cloud layer of aerosols on marine stratocumulus decks, both in the subtropical Atlantic and Pacific. Wilcox (2010) examined CALIPSO lidar and NASA A-Train satellite data over the southeast Atlantic between July to September. They found that aerosol layers can lead to an additional heating of up to 1 K. During periods of high aerosol concentrations above clouds they found that the liquid water path (LWP) increased by up to 20 g m^{-2}. The LWP is the vertically integrated liquid water content between two points in the atmosphere. They also find that the cloud-top altitude for above-cloud smoke was lower by up to 200 m.

In other studies, Costantino and Bréon (2013) examined CALIPSO and MODIS satellite information above the Atlantic, identifying mixed and unmixed cases. Mixed cases occurred when cloud and aerosol layers were adjacent, and unmixed when an above-cloud aerosol layer was present. They found no different in cloud droplet radius sizes with increasing aerosol index for unmixed cases with the sizes remaining at 14-15 μm, also finding no dependence on the LWP. They found a LWP of around 110 g m^{-2} with no aerosols present as well as a positive relationship between aerosols above clouds and cloud fraction which was stronger for low clouds.

Johnson et al. (2004) used a large eddy simulation (LES) model to simulate the semi-direct effect on marine stratocumulus decks, using data collected off the California coast. They concluded that aerosols above the inversion enhanced the LWP and led to a negative semi-direct forcing. In addition they also found a lower entrainment rate and a shallower boundary layer. Similarly Sakaeda et al. (2011) examined the semi-direct and direct effect of southern African biomass burning on the regional scale, using a global atmospheric model, focusing on aerosols above clouds. They found that the semi-direct radiative effects have magnitudes similar to the direct effect. Over the ocean cloud responses are dominated by an increase in cloud cover with little change in LWP. This means that the net top of the atmosphere (TOA) semi-direct effect over oceans is negative (cooling).

Figure 4 gives an overview of the semi-direct cloud-aerosol interaction when aerosols are found above the cloud layer. The effect of an above-cloud layer on cloud microphysical properties can be explained by a strengthening of the inversion layer. Aerosols absorb radiation and warm the layer in which they reside, leading to an enhanced temperature inversion. This increased inversion layer reduces dry air entrainment into the boundary layer, leading to a shallower, moister boundary layer. The enhanced moisture retention within the boundary layer leads to a thickening of the cloud layer and thus the enhanced LWP observed when aerosols overlay a stratocumulus cloud deck. In addition, as the altitude of the cloud top is maintained by a balance of subsidence above the boundary layer and entrainment at cloud-top, the decrease in cloud-top altitude, often observed with above-cloud aerosols, is also caused by the strengthened inversion leading to decreased entrainment from the troposphere (Wilcox, 2010).

Overall it is concluded that the semi-direct effect of aerosol above clouds will lead to a negative radiative forcing. Johnson et al. (2004) gives an estimate of -10 W m^{-2}. Brioude et al. (2009) found an indirect radiative forcing of -7.5% when biomass burning aerosols were vertically separated from marine boundary layer stratocumulus in the Pacific. Wilcox (2010) also find a negative semi-direct radiative forcing that will counteract the positive aerosol warming. However the balance of these opposite radiative forcing effects depends on the amount and optical properties of the aerosol, as well as the thickness and coverage of the cloud deck (Wilcox, 2010).

4.2 Aerosols within clouds: The cloud-albedo effect and semi-direct effect

While the majority of literature observes that cloud and aerosol layers are vertically separated over the southeastern Atlantic, cases where aerosol layers and cloud layer mix may occur over Ascension Island. Swap et al. (1996) found that as aerosol layers are transported from the African coast they undergo subsidence, with parcels arriving at Ascension at heights up to 2 km. Costantino and Bréon (2013) found examples of cloud and aerosol mixing over the southeastern Atlantic in 44% of their cases, with 56% separated cases. In these cases, the aerosols influence on cloud microphysical properties is not limited to the semi-direct effect as is the case when cloud and aerosol layers are separated.

The most well-known cloud-aerosol interaction is the cloud-albedo effect, first discussed by Twomey (1977). The cloud-albedo effect is the increase in the cloud albedo due to an increased aerosol concentration resulting in enhanced cloud droplet numbers and thus higher cloud reflectivity (McComiskey et al., 2009). Secondary effects of this increase in cloud droplet number include a decrease in the size of cloud droplets which can lead to an alteration of the cloud lifetime, suppression of precipitation or an enhancement of evaporation (Boucher et al., 2013). In cases where clouds and aerosols mix, we expect to observe decreases in the effective radius (R_{eff}) of cloud droplets, together with an increase in the droplet number concentration (N_c). Costantino and Bréon (2013) found a decrease in R_{eff} of 30% with increasing aerosol concentrations, down from 15-16 μm to 11 μm. They also noted a decrease in LWP with increasing aerosol concentrations.

In addition to the cloud-albedo effect, the semi-direct effect also occurs when the aerosol and cloud layers mix in the same layer. Hill and Dobbie (2008) used an LES model with cloud microphysics to study the impact of an absorbing layer of aerosols in the boundary layer on marine stratocumulus. They found that a layer of absorbing aerosols within the cloud layer reduced the LWP, cloud-top altitude and increase the cloud-base altitude, resulting in cloud thinning. They also found that the increase in CCN lead to enhanced cloud evaporation and cloud-top entrainment. This enhancement of cloud evaporation is often called "cloud burn-off". For more information on the semi-direct effect,Koch and Del Genio (2010) provide a summary paper, which includes cases of above-cloud and within-cloud aerosol layers. When aerosols and clouds mix, the semi-direct effect is likely to be strong and positive (Johnson et al., 2004).

These cloud responses to aerosols depend not only on the location of the aerosols compared to the clouds, but also depend on the aerosol optical properties (Koch and Del Genio, 2010). We assume that the majority of biomass burning smoke is black carbon and is an absorbing aerosol. These effects also depend on cloud type. Here we are only concerned with marine boundary layer stratocumulus.

5 Method

The ASCII campaign aimed at determining the extent to which the presence of aerosols influence cloud microphysical properties. To observe cloud microphysical properties we used a new method, developed by Donovan et al. (2015). This method utilizes the propensity of light to become depolarized when it undergoes multiple scattering within a liquid water cloud. The backscattered radiation from spherically symmetrical and uniform elements such as liquid cloud droplets retains the polarization of the incident light under single scattering. However, the returning light will be partially depolarized due to multiple scattering within liquid water clouds (Liou and Schotland, 1971). While many

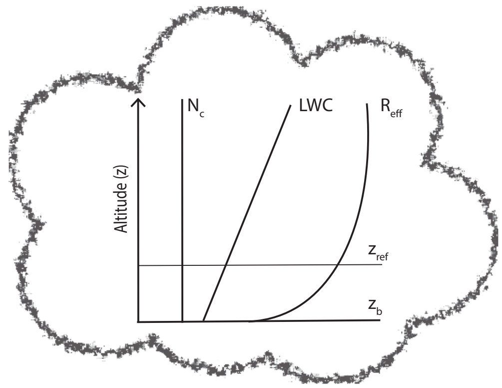

Figure 5: Sketch of the simple cloud model used in the MC modelling to derive LUTS. See Donovan et al. (2015) for a detailed description of the cloud model.

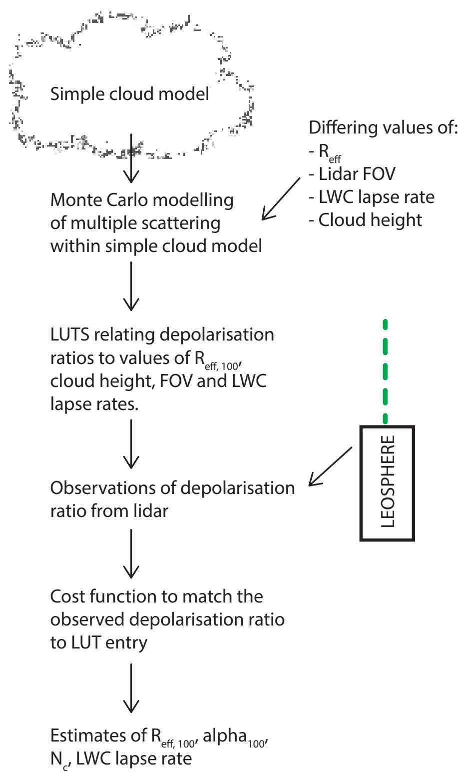

Figure 6: Flowchart of the inversion process for retrieving cloud microphysical properties from the observed depolarisation ratio.

efforts to extract cloud properties from depolarisation ratios of lidars has been undertaken, most of the work with depolarization lidars and clouds has focused on homogeneous clouds which are not very realistic (Donovan et al., 2015).

5.1 Inversion method

The inversion method used here is based on a simple cloud-base representation, with a linear liquid water content lapse rate Γ_l as well as a constant cloud droplet number density N_c (Fig. 5). As the liquid water content (LWC) increases with height while the number density remains constant, this leads to an increase in the R_{eff} with height. The extinction coefficient α also increases with height. The droplet size distribution used is a single-mode modified-gamma distribution. Figure 5 gives an overview of the simple cloud model used. To simplify the cloud model, a reference height z_{ref} of 100 m above the cloud base, is used. This simple cloud model reduces the number of cloud parameters to just two variables; the extinction coefficient, α_{100}, and the effective radius, $R_{\text{eff},100}$, both at 100 m above the cloud base.

Monte Carlo (MC) modelling was then used to simulate multiple scattering within this simple liquid water cloud model. Under single scattering conditions the perpendicular attenuated backscatter (ATB) is much smaller than the parallel ATB (Donovan et al., 2015). However with multiple scattering the perpendicular scattered light can form a much higher proportion of the ATB than predicted by single scattering. The MC modelling used was the Earth Clouds and Aerosols Radiation Explorer (EarthCARE) simulator (ECSIM) lidar-specific MC forward model. MC runs were performed for various values of cloud-base height, lidar field of view (FOV), $R_{\text{eff},100}$ and Γ_l (see Table 1 in Donovan et al. (2015) for exact values).

The aim of the inversion process is then to search within these LUTS to find matches to the lidar observations. To begin the inversion process, the peak of the observed parallel ATB is found for each profile, with each profile then shifted so the observed peaks of parallel ATB match with height. This process of normalising the profiles by the height of the peak parallel ATB avoids the need to accurately identify the cloud base from the observations. This is useful as the cloud base can be difficult to define due to variations in cloud altitude and the presence of sub-cloud drizzle or aerosol particles. The desired number of peaks are then binned and averaged which serves to match the resolution of lidar observations and LUTS. The inversion process then uses a cost function to retrieve the state variables. This cost function (Eq. 25 in Donovan et al. (2015)) requires a priori estimates of the state variables, as well as a priori estimates of the error covariance matrix. The state vector contains values of $R_{\text{eff},100}$ and α_{100} as well as the lidar calibration coefficients. The calibration coefficients are set to a priori estimates (Table 1) while initial estimates of $R_{\text{eff},100}$ and α are found by an initialisation of the minimisation procedure to avoid local minima. In addition, the cost function requires the observation vector (lidar observations), the observations error matrix and a forward vector model which uses values determined by interpolation using the LUTS. The profiles taken from the LUTS

Table 1: Calibration coefficients for the inversion process

Parameter	Value
δ^C	0.013
C_r	37.037
FOV interpolation factor	0.137

are shifted in height given by $\Delta \sin(\phi_{z_p})$, and binned to match the vertical resolution of the observations. Following the initialisation of minimisation process, a two step method is used to minimise the cost function and the resulting values of $R_{\mathrm{eff},100}$ and α_{100} are retrieved. In addition to $R_{\mathrm{eff},100}$ and α_{100}, the inversion process also returns values of C_N, $\Delta \sin(\phi_{z_p})$, the inter-channel depolarisation calibration constant C_r and the polarisation cross-talk parameter δ^c. C_N is a value introduced to account for any error in signal normalisation process. These values are written to a netCDF file. This netCDF file then undergoes further processing to calculate Γ_l and N_c, as well as to complete error propagation calculations. In addition, the inversion process requires temperature and pressure profiles for the periods selected. Here we have used general temperature and pressure profiles for the tropics obtained by the US Air Force Geophysics Laboratory in 1986. However, in further studies it is advisable to use the radiosondes obtained by the ARM Mobile facility (Fig. 10). The ARM Mobile radiosondes are ideal as they were released adjacent by the lidar location 5 times every 24 hours during the ASCII campaign.

While the inversion process does not need the lidar signal to be calibrated absolutely, the process requires the lidar to be calibrated relatively (i.e. calibrated between the parallel and perpendicular channel). As such it is sensitive to the polarisation cross-talk parameter δ^C and the inter-channel depolarisation calibration constant C_r, as well as the lidar field of view FOV. In this study, values of the lidar FOV, δ^C and C_r where not derived for the ASCII campaign specifically with previous estimates of these variables being used instead (Table 1).

An example of the type of observations which were selected for the inversion process is shown in Figure 7. Here the peak parallel ATB is well defined, with no drizzle or sub-cloud aerosols visible. The selection process of deciding which observations to invert was done by eye.

5.2 UV depolarisation lidar

The lidar that was used was a commercial Leosphere ALS-450 lidar operating at 355nm with separate parallel and perpendicular channels. Immediately prior to the ASCII campaign the lidar was serviced by Leosphere. The lidar was set up and tested at Cabauw, Netherlands for around a week, before being shipped to Ascension Island. Figure 8 shows the location of the lidar and the ARM Mobile facility on Ascension Island. The lidar was located next to the UK Met

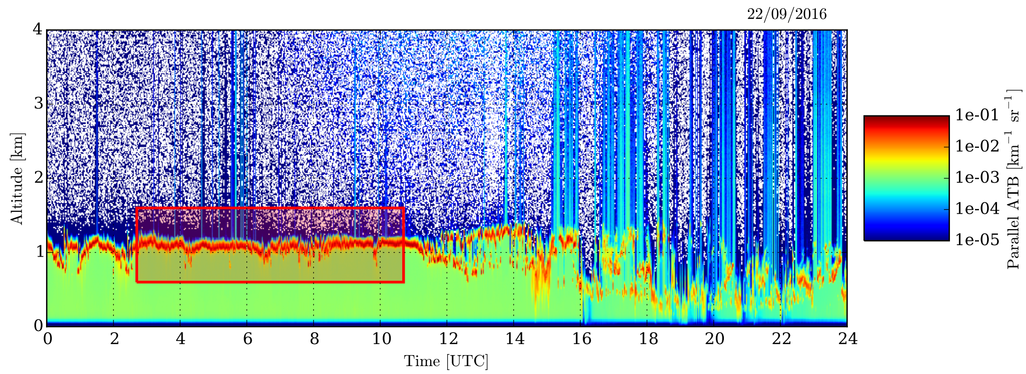

Figure 7: Example of the ideal inversion period (red shaded area). Note the clearly defined cloud base region, as opposed to the conditions later in the day (after 14 UTC).

Office building on the RAF Airbase on Ascension Island (Fig. 9). The lidar was placed approximately 3 m from Met Office building, with the computer and control boxes stored inside and connected through a port in the wall. Also at the Met Office site was an AERONET site, ceilometer and microwave radiometer as well as the release site for ARM radiosondes.

The lidar was operated between the 3^{rd} to the 29^{th} of September. Between 8 UTC on the 24^{th} to 19 UTC 27^{th} the lidar was non-operational due to power cuts at the RAF base and to computer malfunction. The data acquisition software produced ASCII files for each day of observations. These ASCII files were then processed to produce a single netCDF file for each day of observations, as well as additional gif files for quick data visualisation. The netCDF files contain the parallel and perpendicular attenuated backscatter. The data collected has a vertical resolution of around 15m and a temporal resolution of around 30s. Due to the strong background light, the ability to observe aerosols was limited to the night, and to periods when no clouds were present.

6 Results

During the campaign, overcast skies with light drizzle was common. The average surface temperature was 21.32°C, with an average precipitation rate of 0.11 mm hr^{-1} and a wind direction of ESE (Atmospheric Radiation Measurement (ARM) Climate Research Facility, 1993). Generally a well defined stratocumulus deck was present at around 1 to 1.5 km, as well as a persistent temperature inversion (Fig. 10). Due to high solar radiance and the high position of the sun during the day there was a large amount of solar background noise meaning aerosol signals were generally only visible during the night. Aerosols were visible on 19 out of the 25 days observed and occurred between heights of 1.5 to 4.5 km. Days when

Figure 8: Image from Google Maps showing the location of the lidar, given by the yellow cross, and the ARM Mobile Facility site, given by the orange circle, on Ascension Island. Georgetown, the main settlement, and the RAF Airbase are also indicated.

the aerosol layer was observed directly above the cloud base occurred twice as frequently as days when the smoke layer was seen vertically separated above the cloud deck.

6.1 Inversion process

Out of the 25 days that the lidar was operational, 16 of them had periods which were suitable for the inversion process. Figure 11 shows an example of the inversion results for the 22^{nd} of September. On this day the well-defined cloud base region and absence of drizzle resulted in stable inversion products. The N_c is around 1600 cm^{-3} while the $R_{\text{eff},100}$ is about 1.2 μm. Figure 12 shows another example of the inversion products, here for a less well-defined cloud base. Here, the spread of N_c and $R_{\text{eff},100}$ is greater, with the largest scattering associated with potentially drizzling periods.

6.2 Cases

To identify the effects of smoke on cloud properties, each day was classed as either a *clean, mixed* and *separated* case. Appendix B gives a list of which

Figure 9: The lidar in position next to the UK Met Office on Ascension Island. (7°58'10.3"S 14°24'19.8"W)

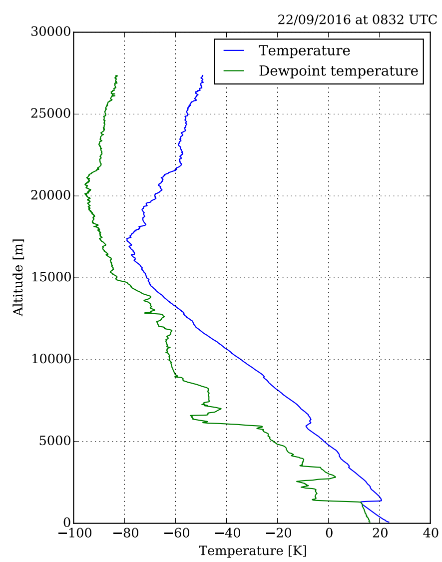

Figure 10: Radiosonde for the 22^{nd} of September at 08:32 UTC, showing the presence of a strong temperature inversion at 1000 m. Taken from Atmospheric Radiation Measurement (ARM) Climate Research Facility (1994) LASIC dataset.

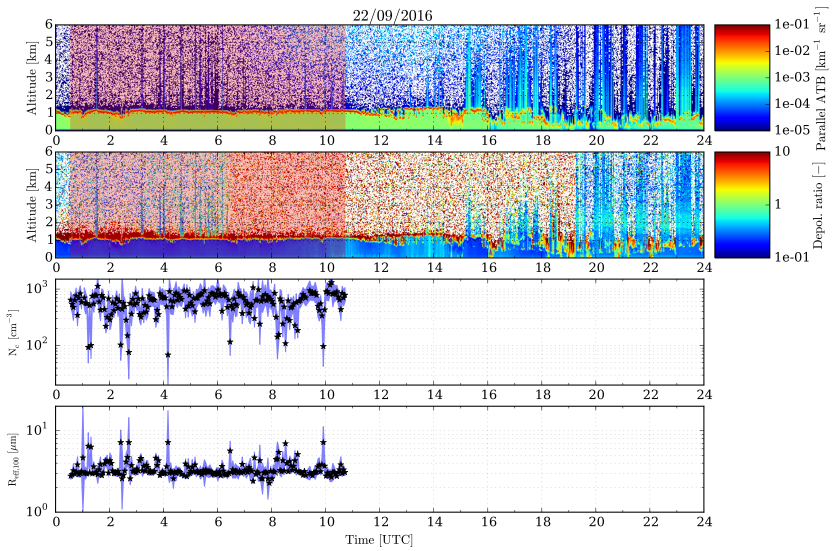

Figure 11: Inversion results for the 22^{nd} of September. This is an example of an ideal period to invert, with a very well-defined ATB peak and an absence of below cloud aerosols or drizzle.

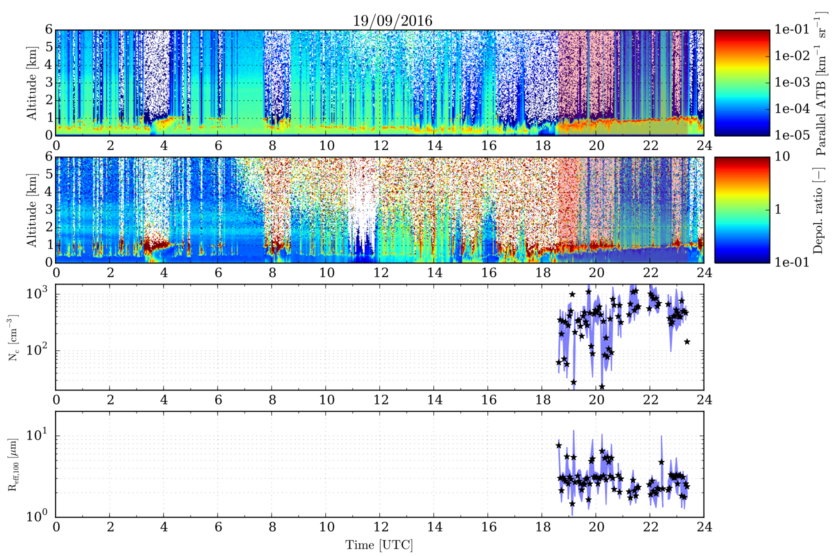

Figure 12: Inversion results for the 19^{th} of September. The potentially precipitating period between 19 to 20 UTC leads to a greater variability in the inversion products.

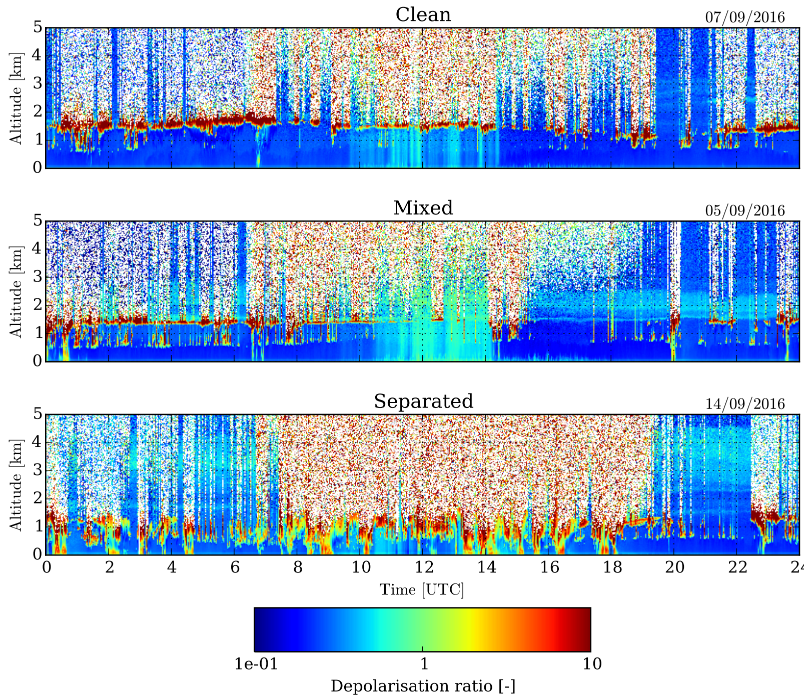

Figure 13: Examples of each of the *clean, mixed* and *separated* cases into which each day was sorted. This selection process was done by eye based on the presence and location of smoke layers.

days fell into what category. *Clean* cases indicates days when no aerosols are visible while *mixed* cases were when aerosols are visible directly above the peak ATB. This indicates that aerosols may have been mixing with the cloud layer. *Separated* cases were days when aerosols are seen in a layer which is vertically separated from the cloud layer below it (Fig. 13). The cases were selected by eye. The majority of days fall in the *mixed* category, with dramatically fewer days falling under the *clean* and *separated* cases (Fig. 14).

The inversion products were averaged for each case (Fig. 15). Generally there is a clear differentiation in the mean values of each inversion product between each of the three cases. However, while the means are divergent, there is still considerable overlap in the mean deviations between the three cases. The $R_{\mathrm{eff},100}$ ranged between 3.4 to 4.2 μm, with the highest value occurring for the *clean* case. Both the *mixed* and *separated* cases had similar mean values for $R_{\mathrm{eff},100}$. The N_c peaked in the *mixed* case at 550 cm^{-3} with the smallest value occurring in the *clean* case.

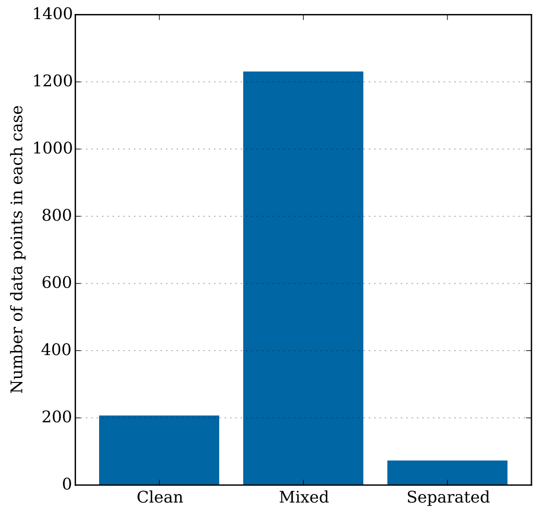

Figure 14: Overview of the number of data points in each different case

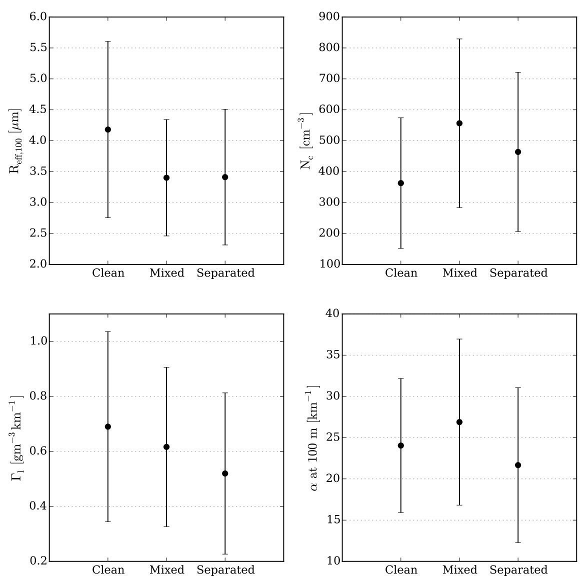

Figure 15: Inversion product averages for each of the three cases. The errorbar indicates the standard deviation.

7 Discussion

It was expected that aerosols over Ascension Island would generally be vertically separated from the clouds (Costantino and Bréon, 2013; Wilcox, 2010). However during this campaign the majority of days fell under the *mixed* case with aerosol layers being visible directly about the peak ATB. This suggests that the aerosols may be mixed into the cloud layer. The presence of aerosols at heights of less than 2 km supports the idea that the widespread subsidence occurring across the southeastern Atlantic region plays a major role in mixing the aerosol layer downwards as it moves away from the African coast, as suggested by Swap et al. (1996).

The *mixed* case shows an increased N_c as well as a smaller $R_{eff,100}$ at 100 m above cloud base. This is assumed to be evidence on the cloud aerosol indirect effect, with aerosol particles acting as CCN. The N_c increased by 200 cm^{-3} from the *clean* case while the $R_{eff,100}$ dropped by almost 1 μm. The separated cases sit in between the clean and mixed for $R_{eff,100}$ and N_c. This may be explained by slight mixing of smoke from the separated layer into the clouds, which is not clearly seen in the lidar. In a previous study over the southeastern Atlantic, Costantino and Bréon (2013) found a drop in $R_{eff,100}$ of 30%, similar to what is observed here (a decrease by 20%). A key difference here is that Costantino and Bréon (2013) were examining satellite observations (cloud top) while the inversion method focuses on cloud properties near the cloud base. In addition other factors which may have lead to this difference between cases, such as varying meteorological conditions, have not been examined in this study.

Here we have not specified any calibration coefficients (i.e. lidar FOV, C_r and δ^C) specifically for the lidar set up on Ascension. The values used here were previously calculated when the lidar was located at Cabauw, Netherlands. Donovan et al. (2015) suggest that to know the R_{eff} to within 10%, C_r should be know to within 5%, while δ^C should be known to within 50%. The inversion process is also sensitive to the lidar FOV although this is considered to be a secondary source of error as the lidar FOV is generally well known. While Donovan et al. (2015) states values of FOV, C_r and δ^C were found to be stable between instrument servicing, prior to being deployed to Ascension Island the lidar was comprehensively serviced by Leosphere due to a breakdown. This may have lead to significant deviations from the calibration coefficients used in this study (Table 1). In addition, δ^C can vary quasi-diurnally by up to 50%, possible due to temperature changes in the lidar unit (Donovan et al., 2015). Donovan et al. (2015) found that the inversion method lead to an estimated error of around 30% in R_{eff}, with a 25% error in N_c when applied to observations taken at Cabauw. Given that the calibration coefficients are better known for Cabauw, the error estimates for the ASCII inversion products are expected to be higher than 30%. Thus using these general estimates of the calibration coefficients leads to very significant uncertainty in the retrieved inversion products. Prior to any further study of the ASCII observations, accurate estimates of FOV, C_r and δ^C for the lidar set up on Ascension should be found, if possible.

A further source of uncertainty in the accuracy of the inversion products is the lack of verification of the inversion method. The inversion method has been applied to lidar observations taken at Cabauw, Netherlands. Here, the retrieved inversion products were not directly compared to observations of cloud microphysical properties. Instead, cloud reflectivity calculated using the inversion products was compared to cloud reflectivity observed with a vertically pointing Doppler radar. While no conclusive validation can be achieved with this comparison, Donovan et al. (2015) stated that the inversion results are physically consistent with the observed radar reflectivity. The inversion-derived Γ_l was also compared to the adiabatic lapse rate Γ_a, calculated using temperature and pressure profiles, with the inversion results not exceeding the adiabatic limit in a statistically significantly manner. A preliminary comparison between cloud base number concentration derived from the inversion results and aerosol number concentration was also performed by Donovan et al. (2015), with the the results being consistent with other independent studies. However, the inversion products have yet to be directly compared with other observations of cloud microphysical properties. Given the wide variety of instruments located at the ARM Ascension site and its close proximity to the ASCII lidar site, these datasets provide an excellent opportunity to verify this inversion method. A potential framework to compare the methods is given in Sarna and Russchenberg (2016), when a ground-based cloud radar and microwave radiometer (MWR) is used to retrieve cloud microphysical properties.

8 Conclusions

The ASCII campaign took place in September 2016 on Ascension Island. A UV depolarisation lidar operating at 355 nm was located on the island to investigate the effect of biomass burning aerosols from Africa on the cloud microphysical properties of the persistent marine stratocumulus clouds which occur over the southeastern Atlantic region. Using a new inversion method, cloud microphysical properties such as the effective radius $\mathrm{R_{eff}}$ and cloud number density N_c could be retrieved from the depolarisation ratio observed by the lidar. Out of the 25 days that the lidar was operating, aerosols were observed on 19, while conditions suitable for the inversion process occurred on 16 days. The results presented here should be treated with caution, as no ASCII-specific lidar calibration coefficients were used. This increases the uncertainty of the inversion products, with uncertainties probably exceeding than 30%. An additional source of uncertainty is the lack of verification of the inversion method itself. For conditions with well defined, non-precipitating cloud decks the inversion method was stable, while it is very sensitive to drizzling conditions or aerosols below the cloud base. The average N_c observed was between 400-600 cm^{-3} while the average $\mathrm{R_{eff}}$ was between 3.4 to 4.2 μm. The observations were classed in three categories; *clean*, *mixed*, *separated* depending on the presence and location of aerosols. There is a clear difference in the N_c and $\mathrm{R_{eff}}$ averages for the *clean* and *mixed* cases. In the *mixed* case the N_c increased while the $\mathrm{R_{eff}}$ decreased compared to the *clean* case, potentially due to the indirect cloud-albedo effect. However, further analysis is required to prove conclusively that is an aerosol-cloud interaction and not due to varying meteorological conditions or inaccuracies in the inversion method.

Appendix A Other campaigns

A.1 LASIC

The Layered Atlantic Smoke Interactions with Clouds (LASIC) campaign is supported by the US Deparment of Energy (DOE). Its aim is to improve our understanding of aged carbonaceous aerosol, its seasonal evolution, and the mechanisms by which clouds adjust to the presence of the aerosol (Zuidema et al., 2016).

Their main observational input is the Atmospheric Radiation Measurement (ARM) Climate Research Facility Mobile Facility (AMF1) which contains is a suite of cloud, aerosol and atmospheric profiling instruments and was deployed on Ascension Island from June 1^{st} 2016 to October 31^{st}, 2017. In addition a more modest secondary instrumentation suite (radar, lidar, spectrometer, AERONET) was placed on St. Helena Island (15^oS 5^oW) through UK-US-DOE cooperation.

A.2 NASA-ORACLES

The National Aeronautic and Space Administration Observations of Aerosols above Clouds and their Interactions (NASA-ORACLES) was also underway during September 2016. ORACLES is a 5 year investigation which began on February 1st 2015. With three deployments periods, the ORACLES mission consists of measuring and modelling direct and semi-direct aerosol effects on climate primarily through aircraft measurements. NASA aircraft with be used to conduct the investigation, flying out of Walvis Bay, Namibia.

A.3 CLARIFY-2016

The UK based Cloud-Aerosol-Radiation Interactions and Forcing (CLARIFY) aimed to bring a wide range of airborne, surface based and satellite measurements of clouds, aerosols and their radiative impacts over the southeast Atlantic. Unfortunately, the CLARIFY campaign was postponed until 2017 (now called CLARIFY-2017).

A.4 AEROCLO-SA

In addition to the US and UK projects, the French Aerosol Radiation and Clouds in Southern Africa (AEROCLO-SA) project, based in Hentjes Bay, north of Walvis Bay, has been taking detailed aerosol column and in-situ measurements since 2012, with plans to continue into the ORACLES and CLARIFY time frame.

Appendix B Separation of days into cases

Table 2: Dates of observations used in each case. Dates in bold indicate observations which were analysed using the inversion method, while the other days had no periods suitable for inversion.

Clean	Mixed	Separated
03/09/16	04/09/16	10/09/16
7/09/16	**5/09/16**	11/09/16
8/09/16	**6/09/16**	**14/09/16**
9/09/16	**12/09/16**	**15/09/16**
17/09/16	**13/09/16**	16/09/16
24/09/16	**18/09/16**	19/09/16
29/09/16	**19/09/16**	27/09/16
	20/09/16	
	21/09/16	
	22/09/16	
	23/09/16	
	28/09/16	

References

Albrecht, B. A., D. A. Randall, S. Nicholls, B. A. Albrecht, D. A. Randall, and S. Nicholls (1988, 6). Observations of Marine Stratocumulus Clouds During FIRE. *Bulletin of the American Meteorological Society 69*(6), 618–626.

Anderson, B. E., W. B. Grant, G. L. Gregory, E. V. Browell, J. E. Collins, G. W. Sachse, D. R. Bagwell, C. H. Hudgins, D. R. Blake, and N. J. Blake (1996, 10). Aerosols from biomass burning over the tropical South Atlantic region: Distributions and impacts. *Journal of Geophysical Research: Atmospheres 101*(D19), 24117–24137.

Atmospheric Radiation Measurement (ARM) Climate Research Facility (1993). *Surface Meteorological Instrumentation (MET), updated hourly.* 7.96696 S 14.34981 W: ARM Mobile Facility (ASI) Ascension Island, South Atlantic Ocean; AMF1 (M1): tmospheric Radiation Measurement (ARM) Climate Research Facility Data Archive: Oak Ridge, Tennessee, USA.

Atmospheric Radiation Measurement (ARM) Climate Research Facility (1994). *Balloon-Borne Sounding System (SONDEWNPN), updated hourly.* 7.96972 S 14.40538 W: ARM Mobile Facility (ASI) Airport Site, Ascension Island, South Atlantic Ocean; Supplemental Site (S1): Atmospheric Radiation Measurement (ARM) Climate Research Facility Data Archive: Oak Ridge, Tennessee, USA.

Bennartz, R. (2007, 1). Global assessment of marine boundary layer cloud droplet number concentration from satellite. *Journal of Geophysical Research 112*(D2), D02201.

Boucher, O., D. Randall, P. Artaxo, C. Bretherton, G. Feingold, P. Forster, V.-M. Kerminen, Y. Kondo, H. Liao, U. Lohmann, P. Rasch, S. Satheesh, S. Sherwood, B. Stevens, and X. Zhang (2013). Clouds and Aerosols. In T. Stocker, D. Qin, G.-K. Plattner, M. Tignor, S. Allen, J. Boschung, A. Nauels, Y. Xia, V. Bex, and P. Midgley (Eds.), *Climate Change 2013: The Physical Science Basis. Contribution of Working Group I to the Fifth Assessment Report of the Intergovernmental Panel on Climate Change.* Cambridge University Press.

Brioude, J., O. R. Cooper, G. Feingold, M. Trainer, S. R. Freitas, D. Kowal, J. K. Ayers, E. Prins, P. Minnis, S. A. Mckeen, G. J. Frost, and E.-Y. Hsie (2009). Effect of biomass burning on marine stratocumulus clouds off the California coast. *Atmos. Chem. Phys. Atmospheric Chemistry and Physics 9*, 8841–8856.

Costantino, L. and F.-M. Bréon (2013, 1). Aerosol indirect effect on warm clouds over South-East Atlantic, from co-located MODIS and CALIPSO observations. *Atmospheric Chemistry and Physics 13*(1), 69–88.

Donovan, D. P., H. Klein Baltink, J. S. Henzing, S. R. de Roode, and A. P. Siebesma (2015, 1). A depolarisation lidar-based method for the determination of liquid-cloud microphysical properties. *Atmospheric Measurement Techniques 8*(1), 237–266.

Fuelberg, H. E., J. D. VanAusdall, E. V. Browell, and S. P. Longmore (1996, 10). Meteorological conditions associated with vertical distributions of aerosols off the west coast of Africa. *Journal of Geophysical Research: Atmospheres 101*(D19), 24105–24115.

Garstang, M., P. D. Tyson, R. Swap, M. Edwards, P. Kållberg, and J. A. Lindesay (1996, 10). Horizontal and vertical transport of air over southern Africa. *Journal of Geophysical Research: Atmospheres 101*(D19), 23721–23736.

Hill, A. A. and S. Dobbie (2008, 7). The impact of aerosols on non-precipitating marine stratocumulus. II: The semi-direct effect. *Quarterly Journal of the Royal Meteorological Society 134*(634), 1155–1165.

Johnson, B. T., K. P. Shine, and P. M. Forster (2004, 4). The semi-direct aerosol effect: Impact of absorbing aerosols on marine stratocumulus. *Quarterly Journal of the Royal Meteorological Society 130*(599), 1407–1422.

Koch, D. and A. D. Del Genio (2010, 8). Black carbon semi-direct effects on cloud cover: review and synthesis. *Atmospheric Chemistry and Physics 10*(16), 7685–7696.

Liou, K.-N. and R. M. Schotland (1971, 7). Multiple Backscattering and Depolarization from Water Clouds for a Pulsed Lidar System. *Journal of the Atmospheric Sciences 28*(5), 772–784.

Lohmann, U. and J. Feichter (2005). Global indirect aerosol effects: a review. *Atmos. Chem. Phys 5*, 715–737.

McComiskey, A., G. Feingold, A. S. Frisch, D. D. Turner, M. A. Miller, J. C. Chiu, Q. Min, and J. A. Ogren (2009, 5). An assessment of aerosol cloud interactions in marine stratus clouds based on surface remote sensing. *Journal of Geophysical Research Atmospheres 114*(9), D09203.

Paluch, I. R., D. H. Lenschow, I. R. Paluch, and D. H. Lenschow (1991, 10). Stratiform Cloud Formation in the Marine Boundary Layer. *Journal of the Atmospheric Sciences 48*(19), 2141–2158.

Roberts, G., M. J. Wooster, and E. Lagoudakis (2009). Annual and diurnal african biomass burning temporal dynamics. *Biogeosciences 6*, 849–866.

Sakaeda, N., R. Wood, and P. J. Rasch (2011, 6). Direct and semidirect aerosol effects of southern African biomass burning aerosol. *Journal of Geophysical Research 116*(D12), D12205.

Sarna, K. and H. W. J. Russchenberg (2016, 3). Ground-based remote sensing scheme for monitoring aerosolcloud interactions. *Atmospheric Measurement Techniques 9*(3), 1039–1050.

Sinha, P., P. V. Hobbs, R. J. Yokelson, D. R. Blake, S. Gao, and T. W. Kirchstetter (2003). Distributions of trace gases and aerosols during the dry biomass burning season in southern Africa. *Journal of Geophysical Research 108*(D17), 4536.

Sinha, P., L. Jaeglé, P. V. Hobbs, and Q. Liang (2004). Transport of biomass burning emissions from southern Africa. *Journal of Geophysical Research 109*(D20), D20204.

Swap, R., M. Garstang, S. A. Macko, P. D. Tyson, W. Maenhaut, P. Artaxo, P. Kållberg, and R. Talbot (1996, 10). The long-range transport of southern African aerosols to the tropical South Atlantic. *Journal of Geophysical Research: Atmospheres 101*(D19), 23777–23791.

Twomey, S. (1977, 7). The Influence of Pollution on the Shortwave Albedo of Clouds. *Journal of the Atmospheric Sciences 34*(7), 1149–1152.

Wilcox, E. M. (2010, 12). Stratocumulus cloud thickening beneath layers of absorbing smoke aerosol. *Atmospheric Chemistry and Physics 10*(23), 11769–11777.

Zuidema, P., C. Chiu, C. Fairall, S. Ghan, P. Kollias, G. McFarguhar, D. Mechem, H. Wang, S. Yuter, M. Alvarado, E. Lewis, S. DeSzoeke, G. Feingold, J. Haywood, D. Turner, A. McComiskey, J. Redemann, R. Wood, D. Romps, and P. Zhu (2016). Layered Atlantic Smoke Interactions with Clouds (LASIC) Science Plan. Technical report, ARM Climate Research Facility.